Ultrafast photoinduced transitions in charge density wave, Mott insulator, and metallic phases of an iodine-bridged platinum compound

K. Kimura,[1] H. Matsuzaki,[1] S. Takaishi,[2] M. Yamashita,[2] and H. Okamoto[1,3,*]
[1]*Department of Advanced Materials Science, University of Tokyo, Kashiwa, Chiba 277-8561, Japan*
[2]*Department of Chemistry, Tohoku University, Sendai 980-8578, Japan*
[3]*CREST, JST, Kawaguchi, Saitama 332-0012, Japan*
(Received 27 November 2008; published 18 February 2009)

Ultrafast photoinduced transitions among three phases—charge density wave (CDW), Mott-Hubbard insulator, and metal—were investigated in an iodine (I)-bridged platinum (Pt) compound by femtosecond reflection spectroscopy. For a weak photoexcitation, CDW phase over 70 Pt sites is converted to Mott-Hubbard phase by one photon. Such large conversion efficiency makes possible the complete and transient transition from CDW to Mott-Hubbard phase. For a strong excitation, the low-energy spectral weight is increased, suggesting a conversion to a metallic state.

DOI: 10.1103/PhysRevB.79.075116 PACS number(s): 78.47.J−, 71.30.+h, 71.45.Lr, 78.40.Ha

I. INTRODUCTION

Phase conversion in solids by a photoirradiation, which is called "photoinduced phase transition," is one of the most attention-gaining phenomena not only in the fields of solid-state physics but also in the field of optical technology.[1] It is because a photoinduced phase transition in an ultrafast time scale may be used as a useful mechanism for future optical switching devices. Several transient photoinduced transitions between nearly degenerate two phases have been reported so far, e.g., insulator-metal transitions in VO_2,[2] the neutral-ionic transition in tetrathiafulvalene-*p*-chloranil,[3,4] the charge-/orbital-order insulator to ferromagnetic metal transition in the manganite,[5–7] the diamagnetic spin-Peierls phase to paramagnetic phase transition in K-tetracyanoquinodimethane,[8,9] and so on. In all of these transient photoinduced transitions, the conversion from one phase to another is not perfect, resulting to coexistence of original phase and the photoinduced phase. When we consider applications of photoinduced transitions to switching devices, a complete but transient transition should be realized in an ultrafast time scale. To achieve this, in the present study, we focus on the halogen (*X*)-bridged transition metal (*M*) compound (the *MX*-chain compound),[10] which is a prototypical one-dimensional (1D) system under strong electron correlation and electron-lattice interaction.

In the *MX*-chain compounds, electronic properties are dominated by 1D chains composed of alternating metal (*M*=Ni, Pd, or Pt) and halogen (*X*=Cl, Br, and I) ions in which purely 1D electronic state is formed by the p_z orbital of *X* and the d_{z^2} orbital of *M*. The nominal valence of *M* is 3+ and an unpaired electron exists in the d_{z^2} orbital. In the Ni compounds, the monovalence state ($\cdots X^{-}$-M^{3+}-X^{-}-M^{3+}-$X^{-}\cdots$) or equivalently the Mott-Hubbard (MH) insulator state is formed because of the large on-site Coulomb repulsion *U*.[11] In the Pd or Pt compound, the monovalence state is unstable due to the strong electron-lattice interaction and instead the charge density wave (CDW) state with dimeric displacements of *X* ($\cdots X^{-}$-M^{4+}-$X^{-}\cdots M^{2+}\cdots X^{-}$-$M^{4+}$-$X^{-}\cdots M^{2+}\cdots X^{-}$-) is stabilized.[12]

In the PdBr-chain compound, $[Pd(chxn)_2Br]Br_2$ (chxn =cyclohexanediamine), located near the CDW-MH phase boundary,[13] the CDW phase is changed to the MH phase by substituting 16% of Pd with Ni.[14] Moreover, the photoinduced CDW to MH conversion was reported.[15] In this photoinduced transition, about half of the CDW is converted to the MH state, but a complete CDW-MH transition has not been achieved.

In this paper, we report on the photoinduced phase transition of the PtI-chain compound, $[Pt(chxn)_2I]I_2$, investigated by a femtosecond pump-probe (PP) reflection spectroscopy. This compound is located very close to the CDW-MH phase boundary.[16] In the PtI chain, the transfer energy between the neighboring *M* ions is larger than that in the PdBr chain, so that the CDW-MH transition will be more continuous[17] and the transition efficiency will be enhanced as compared to the PdBr chain. We indeed demonstrate that the photoinduced CDW-MH transition occurs with high efficiency leading to a complete phase conversion. For a strong photoexcitation, the low-energy spectral weight is increased, which is discussed in terms of the MH insulator to metal transition.

II. EXPERIMENTAL DETAILS

A single crystal of $[Pt(chxn)_2I]I_2$ was grown by the diffusion method according to the previous paper.[16] The femtosecond PP spectroscopy was conducted using a $Ti:Al_2O_3$ regenerative amplifier as a light source. The output from the amplifier (with the energy of 1.55 eV, pulse width of 130 fs, and repetition of 1 kHz) was separated into two beams. One was used for the pump light and the other for the excitation of an optical parametric amplifier, from which the probe lights (0.1–2.5 eV) were obtained. We can adjust the delay time t_d of the probe pulse relative to the pump pulse by changing the length of the route of the pump pulse. The time resolution of the apparatus is 180 fs. All measurements were performed at 293 K.

III. RESULTS AND DISCUSSIONS

Figure 1(a) shows the reflectivity (*R*) spectrum of $[Pt(chxn)_2I]I_2$ with the light polarization (*E*) parallel to the

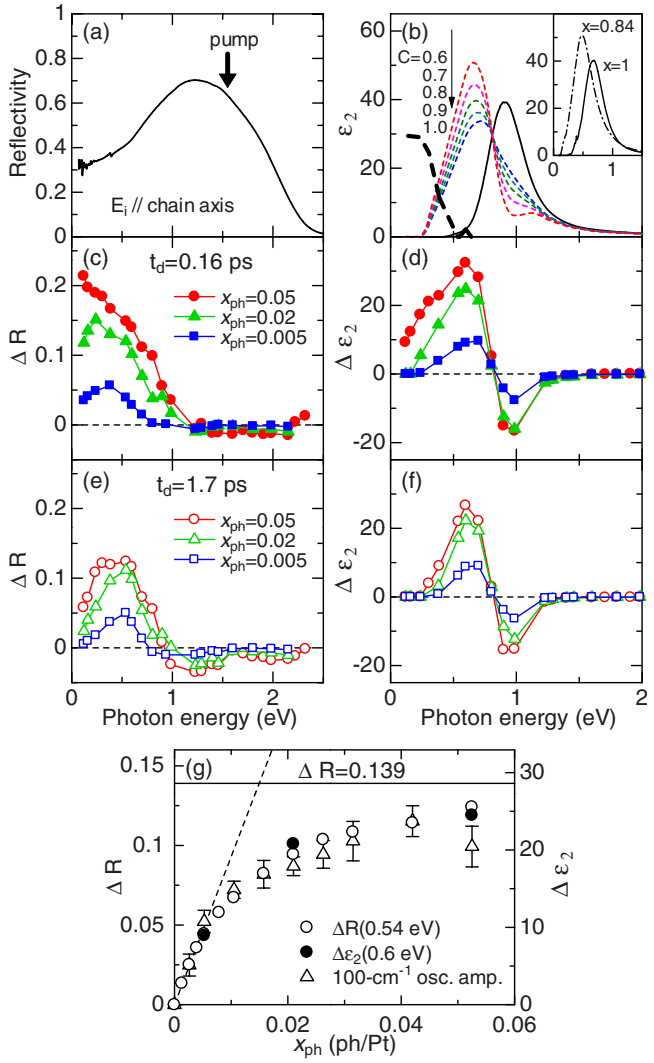

FIG. 1. (Color online) (a) and (b) Polarized reflectivity (R) and ε_2 spectra along the chain (solid lines) in $[Pt(chxn)_2I]I_2$. Thin broken lines in (b) show the ε_2 spectra of the MH state for various C values. The thick broken line shows the ε_2 spectrum for the photoinduced metallic state (see text). The inset in (b) shows the ε_2 spectra of $[Ni_{1-x}Pd_x(chxn)_2Br]Br_2$. (c)–(f) Photoinduced changes in R (ΔR) and ε_2 ($\Delta\varepsilon_2$) for three excitation densities at t_d=0.16 and 1.7 ps. (g) Excitation-density dependence of ΔR (0.54 eV) and $\Delta\varepsilon_2$ (0.6 eV) at t_d=1.7 ps and the amplitude of the coherent oscillation (100 cm^{-1}) on ΔR (0.69 eV) in arbitrary unit. The dashed line shows a linear relation.

chain axis **b** ($E\|\mathbf{b}$). The imaginary part of dielectric constant (ε_2) [solid line in panel (b)] was obtained by using the Kramers-Kronig transformation (KKT) of the R spectrum and the Roessler correction.[18] The broad peak at 0.95 eV is due to the charge-transfer (CT) transition $(Pt^{2+},Pt^{4+}) \rightarrow (Pt^{3+},Pt^{3+})$. In Figs. 1(c) and 1(e), photoinduced reflectivity changes (ΔR) spectra for $E\|\mathbf{b}$ with the polarization of the pump light $E_{ex}\|\mathbf{b}$ are presented for three excitation densities (x_{ph}). x_{ph} is the averaged photon (ph) density of the pump light absorbed within the absorption depth (~300 Å). The delay time t_d of the probe light relative to the pump light is 0.16 and 1.7 ps. Errors of ΔR are smaller than 10^{-3} (10^{-4}) in the mid-IR (near-IR) region. At t_d=0.16 ps, the reflectivity increases below 1 eV. For x_{ph}=0.005 and 0.02 ph/Pt, ΔR has a peak at ~0.4 eV, while for x_{ph}=0.05 ph/Pt, ΔR has no peak but monotonically increases with decrease in energy. At t_d=1.7 ps, ΔR has a peak at ~0.4 eV in common. The results suggest that there is a metastable photoinduced phase characterized by the reflection peak at ~0.4 eV.

To get information of the photoinduced phase, the photoinduced change in ε_2 ($\Delta\varepsilon_2$) [Figs. 1(d) and 1(f)] was obtained by KKT of $(R+\Delta R)$.[19] At t_d=0.16 ps, ε_2 decreases at ~0.95 eV in common. For x_{ph}=0.005 and 0.02 ph/Pt, ε_2 rather increases at ~0.6 eV. Such spectral changes are very similar to those observed in the CDW-MH transition of the PdBr chains,[15] indicating that the similar transition occurs in the PtI chains. For x_{ph}=0.05 ph/Pt, $\Delta\varepsilon_2$ has a large spectral weight below 0.2 eV, suggesting a formation of a metallic state. At t_d=1.7 ps [Fig. 1(f)], the spectral shape of $\Delta\varepsilon_2$ is equal to that for x_{ph}=0.005 and 0.02 ph/Pt at t_d=0.16 ps. This indicates that the metallic state quickly returns to the MH state.

Here we evaluate the CDW-MH transition efficiency Φ. In Fig. 1(g), the magnitude of $\Delta\varepsilon_2$ at 0.6 eV, $\Delta\varepsilon_2$ (0.6 eV), characterizing the amount of the MH state is plotted by solid circles for three x_{ph} values. The excitation density dependence of ΔR at 0.54 eV, ΔR (0.54 eV), is also shown by open circles, which coincides with that of $\Delta\varepsilon_2$ (0.6 eV). Therefore, we use ΔR (0.54 eV) as a measure for the amount of the MH state. ΔR (0.54 eV) is proportional to x_{ph} for the low excitation density [the broken line in Fig. 1(g)]. It starts to deviate from the linear relation at x_{ph} ~0.006 ph/Pt and tends to saturate for $x_{ph}>0.015$ ph/Pt. Such saturation is attributable to the space filling of the photogenerated species.[8,20,21] Assuming the space filling of the photoinduced MH states and the saturation density of x_{ph} =0.015 ph/Pt, Φ is evaluated to be 70 Pt sites/ph. In $[Pd(chxn)_2Br]Br_2$, ΔR is proportional to x_{ph} at least up to 0.025 ph/Pd which is about 4 times as large as 0.006 ph/Pt and Φ (~20 Pd sites/ph) is about 1/3.5 of 70 Pt sites/ph in the PtI compound.[15] These results are fairly consistent with each other. Using the value of Φ and the linear relation between ΔR and x_{ph}, we can evaluate the ΔR value for the complete CDW to MH conversion to be 0.139, which was shown by the solid line in Fig. 1(g). From this line, the ratio C of the photoinduced MH state relative to the original CDW state for x_{ph}=0.05 is estimated to be 0.9.

We can deduce the reflectivity spectrum for the MH state using a C value. Thin broken lines in Fig. 1(b) show the spectra of $\varepsilon_2(\text{CDW})+\Delta\varepsilon_2$ (0.05)/C with C=0.6–1.0, which give the hypothetical spectra of the MH phase. Here, ε_2 (CDW) is the original spectrum and $\Delta\varepsilon_2$ (0.05) is $\Delta\varepsilon_2$ at t_d=1.7 ps for x_{ph}=0.05 ph/Pt. In the inset of Fig. 1(b), the ε_2 spectrum of $[Ni_{0.16}Pd_{0.84}(chxn)_2Br]Br_2$ in the MH phase is presented together with that of $[Pd(chxn)_2Br]Br_2$ in the CDW phase.[14] The former provides a single peak with a Lorentzian shape. Therefore, it is reasonable to consider that the C values of 0.6–0.8 giving the split or distorted spectra are not valid and the appropriate C value is 0.9–1.0. This is also consistent with the C value (0.9) estimated from the excitation density dependence.

To clarify the nature of the metallic state produced just after the photoirradiation for x_{ph}=0.05 ph/Pt, we normalized

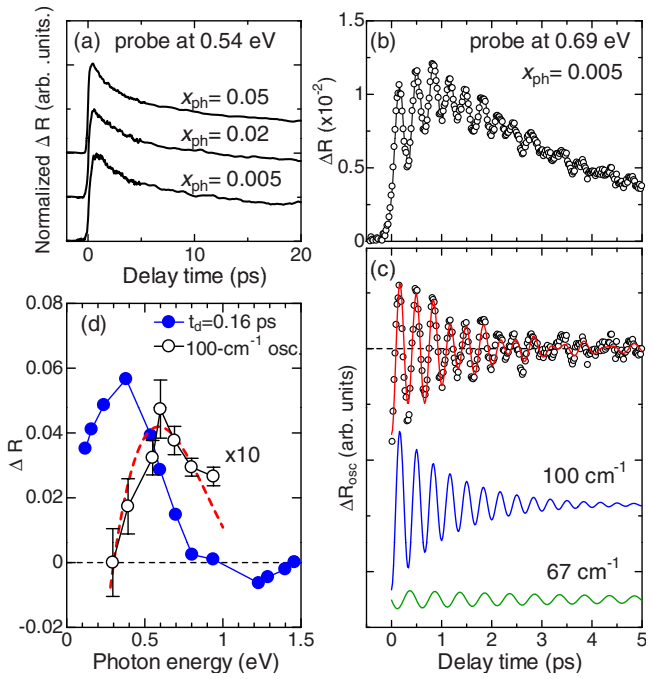

FIG. 2. (Color online) (a) Time profiles of normalized ΔR (0.54 eV). (b) Time profile of ΔR (0.69 eV) for x_{ph}=0.005. (c) Oscillatory components extracted from (b) and the fitting curve (solid line) which is the sum of the two damped oscillators shown in the lower part. (d) Probe-energy dependence of the 100 cm^{-1} oscillation amplitude (open circles) and ΔR (t_d=0.16 ps) (solid circles) for x_{ph} =0.005 ph/Pt. The broken line is the first derivative of ΔR (t_d =0.16 ps).

the $\Delta\varepsilon_2$ spectra for x_{ph}=0.05 and 0.02 ph/Pt (t_d=0.16 ps) at the absorption peak (0.65 eV) for the MH state and calculated the differential spectrum between them, which is shown by the thick broken line in Fig. 1(b). The spectrum shows a monotonous increase with decrease in energy, demonstrating the formation of a metallic state. As discussed above, the conversion to the MH state is almost complete for x_{ph} =0.05 ph/Pt. It is therefore natural to consider that the metallic state is produced by the carrier doping to the MH state. Such a carrier doping may be understood possibly by the following processes: (1) the residual CDW domains or the boundary between the MH domains has finite charges, acting as additional carriers in the MH state or (2) the MH state is formed by the first half of the pump pulse and the carriers are generated in the MH state by the second half of the pump pulse, while it is difficult to discriminate these two processes.

Let us proceed to the discussion about the dynamics of the photoinduced phase transition. In Fig. 2(a), the time profiles of normalized ΔR (0.54 eV) are presented. The signal instantaneously rises, indicating that the MH domain is formed within the time resolution. The decay time of the MH domain is ~20 ps. These features are independent of x_{ph}. Subsequently to the initial rise, the coherent oscillations are observed. To scrutinize the oscillations, we selected ΔR (0.69 eV) for x_{ph}=0.005 ph/Pt, which is plotted in Fig. 2(b), and extracted the oscillatory component by subtracting the background rise and decay from ΔR, which is plotted in Fig. 2(c). The oscillatory component can be reproduced by the sum of the two damped oscillators,

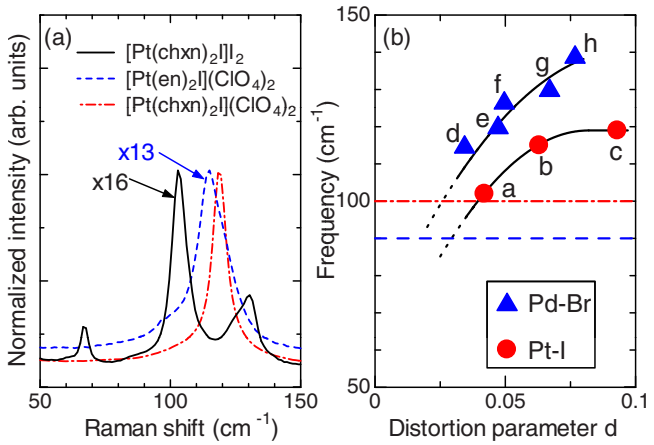

FIG. 3. (Color online) (a) Polarized Raman spectra obtained from a 1.96 eV excitation for [Pt(chxn)$_2$I]I$_2$, [Pt(en)$_2$I](ClO$_4$)$_2$, and [Pt(chxn)$_2$I](ClO$_4$)$_2$. (b) Frequencies of the *M*-*X* stretching Raman bands as a function of the distortion parameter *d*; a: [Pt(chxn)$_2$I]I$_2$, b: [Pt(en)$_2$I](ClO$_4$)$_2$, c: [Pt(chxn)$_2$I](ClO$_4$)$_2$, d: [Pd(en)$_2$Br](C$_5$-Y)$_2$, e: [Pd(chxn)$_2$Br]Br$_2$, f: [Pd(en)$_2$Br](C$_5$-Y)$_2$, g: [Pd(en)$_2$Br](C$_4$-Y)$_2$, and h: [Pd(en)$_2$Br](ClO$_4$)$_2$ (en =ethylenediamine and Y=sulfosuccinate) (a–c and e–h: 293 K and d: 206 K). The broken line and the dashed dotted line show the frequency of the coherent oscillation for [Pd(chxn)$_2$Br]Br$_2$ and [Pt(chxn)$_2$I]I$_2$, respectively.

$$\Delta R_{\rm osc} = \sum_i A_i \cos(\omega_i t - \phi_i)\exp(-t/\tau_i) \quad (i = 1,2) \qquad (1)$$

as shown by the solid line. Here, ω_i is the oscillation frequency, τ_i is the decay time, and ϕ_i is the initial phase. In the fitting procedure, the response function of the measurement system was taken into account as a Gaussian profile. The two oscillatory components are also shown in Fig. 2(c). The evaluated ω_i, τ_i, and ϕ_i are 100 cm^{-1}, 1.2 ps, and π (cosine type) for the high-frequency component and 67 cm^{-1}, 5 ps and $3\pi/2$ (sine type) for the low-frequency one. The excitation-density dependence of the amplitude for the 100 cm^{-1} oscillation [triangles in Fig. 1(g)] is the same as that of the amount of the MH phase characterized by ΔR (0.54 eV) (open circles). In addition, the oscillation is of cosine type. These results suggest that the 100 cm^{-1} oscillation is a displacive-type oscillation associated with the CDW-MH transition. Since this transition should be accompanied by the release of the displacements of the I ions, the oscillation can be assigned to the Pt-I stretching mode in the photogenerated MH domains. As the 67 cm^{-1} oscillation is of sine type, it will be due to an impulsive stimulated Raman process.

To clarify the origin for the coherent oscillation with 100 cm^{-1} in more detail, we refer to the Raman spectra. In Fig. 3(a), the Raman spectrum of [Pt(chxn)$_2$I]I$_2$ is presented together with those of other PtI chains, [Pt(en)$_2$I](ClO$_4$)$_2$ and [Pt(chxn)$_2$I](ClO$_4$)$_2$. A small peak at 67 and 130 cm^{-1} in [Pt(chxn)$_2$I]I$_2$ can be assigned to the oscillation of the ligand molecules like the case of [Pd(chxn)$_2$Br]Br$_2$.[15] The bands at 100–120 cm^{-1} are due to the symmetric Pt-I stretching mode. In Fig. 3(b), the frequency of this mode is plotted as a

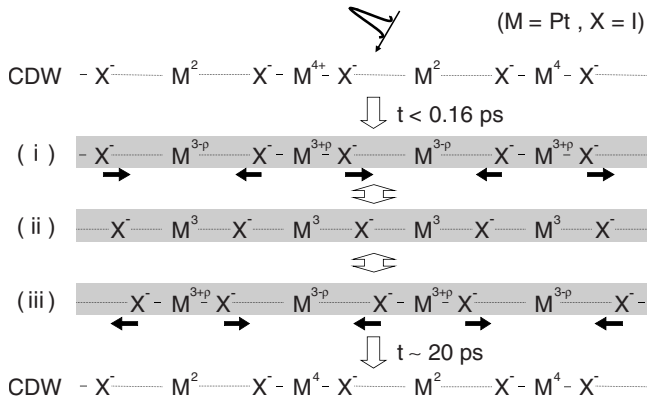

FIG. 4. Schematic of the CDW-MH conversion. After the formation of a 1D M^{3+} domain shown in (i), the equilibrium position of X comes on the midpoint between the neighboring M ions as shown in (ii). At the same time, the coherent oscillation of X occurs as (i)→(ii)→(iii)→(ii)→(i). ρ corresponds to the charge modulation associated with the displacements of X.

function of the distortion parameter d by the solid circles. d is defined as $d=2\delta/L$ (δ is the displacement of the bridging X ions and L is the M-M distance). The frequency of the Pd-Br stretching mode in the PdBr chains was also presented by the solid triangles in the same figure. The frequency of each mode sharply decreases with decrease in d. In fact, in $[Pd(chxn)_2Br]Br_2$, the frequency of the coherent oscillation (90 cm^{-1}) within the photogenerated MH domains [broken line in Fig. 3(b)] is much lower than that of the Pd-Br stretching Raman band [120 cm^{-1}: e in Fig. 3(b)].[15] In $[Pt(chxn)_2I]I_2$, however, the frequency of the coherent oscillation [100 cm^{-1}: dashed-dotted line in Fig. 3(b)] is almost equal to that of the Raman band (102 cm^{-1}) and is larger than that (90 cm^{-1}) in the PdBr chains, although the mass of I is much larger than that of Br.

This contradiction can be explained as follows. Since the size of a photogenerated MH domain is very large (~70 Pt sites) in $[Pt(chxn)_2I]I_2$, the equilibrium position of the bridging I ion should be the midpoint between the neighboring Pt^{3+} ions. In such a case, the frequency of the coherent oscillation on ΔR is double the frequency of the Pt-I stretching vibration. It is because the two electronic states corresponding to phase=π and phase=0 of the oscillation, which are illustrated in Fig. 4(i) and Fig. 4(iii), respectively, are the same with each other.[8] Judging from the relation in Fig. 3(b), the vibrational frequency for $d=0$ should be much smaller than 100 cm^{-1} and may be decreased to ~50 cm^{-1} in the Pt-I chain. In this case, the frequency of the coherent oscillation on ΔR is ~100 cm^{-1} as observed. In $[Pd(chxn)_2Br]Br_2$, in which the size of a MH domain is not so large (~20 Pd sites), the Br ions do not come on the midpoints and therefore the frequency of the coherent oscillation on ΔR is not doubled.

The probe-energy dependence of the 100-cm^{-1}-oscillation amplitude was plotted by open circles in Fig. 2(d). The spectrum is similar not to ΔR (t_d=0.16 ps) (solid circles) but to the first derivative of ΔR (t_d=0.16 ps) (broken line). It indicates that the gap energy in the MH state is modulated by the Pt-I stretching vibration. This also supports the fact that the coherent Pt-I vibrations are generated over the MH state.

From these discussions, the CDW-MH transition dynamics by the weak excitation is illustrated as Fig. 4. By the photoirradiation, a large 1D MH domain (~70 Pt^{3+} sites) is formed from a CT excited state within the time resolution (i). Subsequently, the equilibrium positions of the I ions come on the midpoints between the neighboring Pt ions (ii). At the same time, the coherent vibration of the I ions is generated as (i)→(ii)→(iii)→(ii)→(i)→(ii). The photogenerated MH domain returns to the CDW ground state with ~20 ps.

IV. SUMMARY

We have studied the photoinduced transition from the CDW phase to the MH phase in $[Pt(chxn)_2I]I_2$ by the femtosecond pump-probe reflection spectroscopy. The results have demonstrated the high efficiency of the photoinduced CDW-MH transition in which ~70 Pt sites are converted to MH state per photon. In the photogenerated MH domains, the bridging I ions come on the midpoints between the neighboring Pt ions. With increase in the excitation density, the CDW-MH transition is completed and the transition to the metallic state occurs. Such complete and ultrafast transient phase conversion will be a key mechanism for future optical switching devices using photoinduced phase transitions.

ACKNOWLEDGMENTS

The authors thank K. Yonemitsu and K. Iwano for many enlightening discussions. This work was supported in part by MEXT (16076207 and 20110005) and JSPS (20340072).

*Corresponding author; okamotoh@k.u-tokyo.ac.jp

[1] *Photoinduced Phase Transitions*, edited by K. Nasu (World Scientific, Singapore, 2004).
[2] A. Cavalleri, Cs. Toth, C. W. Siders, J. A. Squier, F. Raksi, P. Forget, and J. C. Kieffer, Phys. Rev. Lett. **87**, 237401 (2001).
[3] S. Koshihara, Y. Tokura, T. Mitani, G. Saito, and T. Koda, Phys. Rev. B **42**, 6853 (1990).
[4] S. Iwai, Y. Ishige, S. Tanaka, Y. Okimoto, Y. Tokura, and H. Okamoto, Phys. Rev. Lett. **96**, 057403 (2006).
[5] M. Fiebig, K. Miyano, Y. Tomioka, and Y. Tokura, Appl. Phys. B **71**, 211 (2000).
[6] M. Rini, R. Tobey, N. Dean, J. Itarani, Y. Tomioka,Y. Tokura, R. W. Schoenlein, and A. Cavalleri, Nature (London) **449**, 72 (2007).
[7] M. Matsubara, Y. Okimoto, T. Ogasawara, Y. Tomioka, H. Okamoto, and Y. Tokura, Phys. Rev. Lett. **99**, 207401 (2007).
[8] H. Okamoto, K. Ikegami, T. Wakabayashi, Y. Ishige, J. Togo, H. Kishida, and H. Matsuzaki, Phys. Rev. Lett. **96**, 037405 (2006).

[9] K. Ikegami, K. Ono, J. Togo, T. Wakabayashi, Y. Ishige, H. Matsuzaki, H. Kishida, and H. Okamoto, Phys. Rev. B **76**, 085106 (2007).
[10] M. B. Robin and P. Day, in *Advances in Inorganic Chemistry and Radiochememisty*, edited by H. J. Emeleus (Academic Press, New York, 1967), Vol. 10, p. 217.
[11] K. Toriumi, Y. Wada, T. Mitani, S. Bandow, M. Yamashita, and Y. Fujii, J. Am. Chem. Soc. **111**, 2341 (1989).
[12] For a review, see H. Okamoto and M. Yamashita, Bull. Chem. Soc. Jpn. **71**, 2023 (1998).
[13] H. Okamoto, K. Toriumi, T. Mitani, and M. Yamashita, Phys. Rev. B **42**, 10381 (1990).
[14] H. Matsuzaki, K. Iwano, T. Aizawa, M. Ono, H. Kishida, M. Yamashita, and H. Okamoto, Phys. Rev. B **70**, 035204 (2004).
[15] H. Matsuzaki, M. Yamashita, and H. Okamoto, J. Phys. Soc. Jpn. **75**, 123701 (2006).
[16] S. Takaishi, D. Kawakami, M. Yamashita, M. Sasaki, T. Kajiwara, H. Miyasaka, K. Sugiura, Y. Wakabayashi, H. Sawa, H. Matsuzaki, H. Kishida, H. Okamoto, H. Watanabe, H. Tanaka, K. Marumoto, H. Ito, and S. Kuroda, J. Am. Chem. Soc. **128**, 6420 (2006).
[17] S. Nasu, J. Phys. Soc. Jpn. **52**, 3865 (1983).
[18] D. M. Roessler, Br. J. Appl. Phys. **16**, 1119 (1965).
[19] For the higher-energy region ($\geq$2.5 eV), ΔR is negligibly small, so that we set $(R+\Delta R)=R$. R was measured up to 5 eV, above which we assumed that R was constant.
[20] L. Rothberg, T. M. Jedju, S. Etemad, and G. L. Baker, Phys. Rev. B **36**, 7529 (1987).
[21] H. Okamoto, Y. Ishige, S. Tanaka, H. Kishida, S. Iwai, and Y. Tokura, Phys. Rev. B **70**, 165202 (2004).